Progress in Neuropsychopharmacology & Biological Psychiatry 136 (2025) 111174

Contents lists available at ScienceDirect

Progress in Neuropsychopharmacology & Biological Psychiatry

journal homepage: www.elsevier.com/locate/pnp

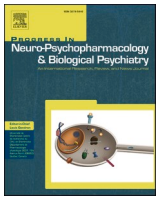

Prenatal ethanol exposure impairs hippocampal plasticity and cognition in adolescent mice

Lorenzo Curti [a], Beatrice Rizzi [b], Francesca Mottarlini [b], Elisabetta Bigagli [a], Alice Ilari [a], Alessia Costa [a], Virginia Sordi [a,d], Giuseppe Ranieri [a], Cristina Luceri [a], Nazzareno Cannella [d], Massimo Ubaldi [d], Alessio Masi [a], Fabio Fumagalli [b], Lucia Caffino [b], Guido Mannaioni [a], Elisabetta Gerace [a,c,*]

[a] Department of Neurosciences, Psychology, Drug Research and Child Health, University of Florence, Florence, Italy
[b] Department of Pharmacological and Biomolecular Sciences, Università degli Studi di Milano, Italy, University of Florence, Florence, Italy
[c] Department of Health Sciences, University of Florence, Florence, Italy
[d] School of Pharmacy, Pharmacology Unit, Centre for Neuroscience, University of Camerino, Via Madonna delle Carceri 9, 62032 Camerino, Italy

ARTICLE INFO

Keywords:
Prenatal alcohol exposure
AMPA
hippocampus
Adolescent mice
microRNA

ABSTRACT

Background: Prenatal alcohol exposure (PAE) induces a wide range of neurodevelopmental disabilities that are grouped under the term 'fetal alcohol spectrum disorders' (FASD). The effects of PAE on brain development are dependent on complex neurochemical events, including modification of AMPA receptors (AMPARs). We have recently found that chronic ethanol (EtOH) exposure decreases AMPA-mediated neurotransmission and expression through the overexpression of the specific microRNA (miR)137 and 501-3p, which target GluA1 AMPA subunit, in the developing hippocampus in vitro. Here, we explored how PAE mice may alter AMPAergic synapses in the hippocampus, and its effects on behavior.

Methods: To model PAE, we exposed C57Bl/6 pregnant mice to 10 % EtOH during during the first 10 days of gestation (GD 0–10; equivalent to the first trimester of pregnancy in humans). AMPA subunits postsynaptic expression in the hippocampus, electrical properties of CA1 neurons, memory recognition, and locomotor functions were then analyzed in adolescent PAE-exposed offspring.

Results: PAE adolescent mice showed dysregulation of AMPAergic neurotransmission, and increased miR 501-3p expression, associated with a significant reduction of spontaneous AMPA currents and intrinsic somatic excitability. In addition, PAE reduced the phosphorylation of AMPAR-containing GluA1 subunit, despite an increase in its total levels. Of note, the total levels of GluA2 and GluA3 AMPA receptors were enhanced as well. Consistently, at behavioral level, PAE reduced object recognition without altering locomotor activity.

Conclusions: Our study shows that PAE leads to dysfunctional formation of AMPAergic synapses that could be responsible for neurobehavioral impairments, contributing to the understanding of the pathogenesis of FASD.

1. Introduction

Prenatal alcohol exposure (PAE) affects brain development, increasing the risk for negative outcomes that persist into adulthood, resulting in delayed neurodevelopment and impairment of cognitive functions including mental retardation (Charness et al., 2016; O'Leary et al., 2013). Since there is no safe amount level of PAE (Charness et al., 2016), the international guidelines recommend zero alcohol during pregnancy (National Health and Medical Research Council, 2020). However, recent epidemiological studies report that about 10 % of pregnant women are exposed to alcohol worldwide (Popova et al., 2018, Popova et al., 2017) causing the occurrence of birth defects grouped under the term fetal alcohol spectrum disorders (FASD). FASD is a global public health problem, with an estimated prevalence in the general population of about 1–2 cases per 1000 individuals (1 % to 20 % among children) (May et al., 2015; Popova et al., 2023). PAE can interfere with both embryonic and fetal development, producing a wide range of outcomes, such as characteristic facial dysmorphology, growth

* Corresponding author at: Department of Health Sciences, Section of Clinical Pharmacology and Oncology, University of Florence, Viale Pieraccini 6, 50139 Florence, Italy.
E-mail address: elisabetta.gerace@unifi.it (E. Gerace).

https://doi.org/10.1016/j.pnpbp.2024.111174
Received 21 June 2024; Received in revised form 14 October 2024; Accepted 14 October 2024
Available online 22 October 2024

deficiencies, neurocognitive deficits, self-regulatory and adaptive function impairments (Anthony et al., 2010; Bower et al., 2013; Lisdahl et al., 2013; Mattson et al., 2011; Murawski et al., 2015; Norman et al., 2009; Spadoni et al., 2007). These effects largely depend on the pattern of exposure, which varies based on the amount, frequency, duration and timing of exposure (Wozniak et al., 2019). Studies on animals indicated that ethanol (EtOH)-induced facial dysmorphology patterns are correlated and depend on the level of EtOH exposure (Lipinski et al., 2012), particularly during the initial gestational period (Godin et al., 2010; Kietzman et al., 2014; Sulik et al., 1981).

The effects of PAE on brain development rely on multiple mechanisms, including glutamate neurotransmission and mitochondrial function, disruption of neuronal-glial interactions (Darbinian et al., 2021; Rubert et al., 2006), and inflammatory changes (Kane and Drew, 2021), which are particularly vulnerable to alterations during the developmental stage. Additionally, PAE may promote alteration of epigenetic gene regulation and selected microRNAs (miRNAs) expression (Cantacorps et al., 2019; Gutherz et al., 2022; Mews et al., 2019). Exposure to EtOH during key stages of fetal development can lead to significant alterations in miRNA expression profiles, contributing to the pathophysiology of FASD. For example, studies have identified the downregulation of miRNAs such as miR-21, miR-9, and miR-153 in response to EtOH exposure, which can interfere with normal neuronal development and function (Sathyan et al., 2007; Balaraman et al., 2013). Moreover, decreased expression of miR-335 and miR-9 has been reported in developing PAE fetus (Sathyan et al., 2007), while brain upregulation of miR-26b induced by PAE has shown also to target the cannabinoid receptor 1 (Stringer et al., 2013). Moreover, other reports have revealed that these miRNA changes can impair critical processes like neurogenesis, synaptic plasticity, and neural network formation (Pappalardo-Carter et al., 2013; Tsai et al., 2014). Interestingly, long term alcohol consumption by fathers also affects the offsprings mental health (Ricci et al., 2017; Anifandis et al., 2014). Collectively, these effects result in altered neural circuits and decreased neuronal plasticity that are responsible for mental defects in adulthood. Nowadays, there is no cure for FASD children, and the exploration of the brain mechanisms altered in response to PAE becomes fundamental to better understanding how homeostatic imbalance and different long-term neurobehavioral impairments become manifest.

Interestingly, the role of AMPA receptors (AMPARs) was recently highlighted in PAE-induced brain alterations. In fact, fetal EtOH exposure leads to decreased AMPA receptor-mediated synaptic transmission in CA1 neurons (Bellinger et al., 2002; Puglia and Valenzuela, 2009; Wijayawardhane et al., 2007). Moreover, it has been shown that aniracetam, an allosteric modulator of AMPARs, improves AMPAR-mediated neurotransmission and reverses learning and memory deficits induced by PAE in adolescent rats (Vaglenova et al., 2008; Wijayawardhane et al., 2008, Wijayawardhane et al., 2007). However, the mechanisms underlying EtOH-induced changes in AMPAR functionality are poorly investigated. In this regard, we recently proposed a mechanism by which EtOH alters the expression of AMPA (Gerace et al., 2023, Gerace et al., 2016). Specifically, immature organotypic hippocampal slices displayed downregulation of postsynaptic AMPARs, through a mechanism involving mGlu5-dependent translational repression of the AMPA subunit GluA1 and the upregulation of miR 137 and 501-3p that specifically target GluA1.

In the present paper, we examined the effects of PAE on hippocampal AMPAR functionality in C57Bl/6 adolescent mice from a molecular, electrophysiological and behavioral point of view. To this end, we generated an in vivo model of PAE based on the literature (Kaminen-Ahola et al., 2010b, Kaminen-Ahola et al., 2010a; Petrelli et al., 2018), in order to resemble alcohol consumption during gestation in women. Indeed, the drinking patterns observed in among 10 % of pregnant women worldwide (Popova et al., 2017) indicate that around 54 % drink during the first trimester, when women may not know they are pregnant or have unplanned pregnancies (Muggli et al., 2016), thus making the first gestational period at high risk of harmful PAE. Therefore, C57Bl/6 pregnant mice were exposed to 10 % EtOH during gestation and AMPA subunits protein postsynaptic expression, electrical properties of CA1 neurons, recognition memory, and locomotor functions were then analyzed in the hippocampus of adolescence offspring.

2. Materials and methods

Male and female C57Bl/6 mice were obtained from Charles River (MI, Italy). Animals were housed at 23 ± 1 °C under a 12 h light-dark cycle (lights on at 07:00). Standard laboratory diet and tap water were provided ad libitum. The experimental protocol was approved by the Italian Ministry of Health (Authorization number 545/2018) and adhered to the European Communities Council Directive 2010/63/EU for the use of laboratory animals.

2.1. Materials

Unless otherwise specified, reagents were purchased from Merck (Saint-Louis, MO, USA). The following NMDA and GABA antagonists were used: D/L-APV (50 μM) and Gabazine (10 μM; Tocris Bioscience, Bristol, UK). For electrophysiological experiments, all drugs were diluted from 100 to 1000× stock solutions to the final concentration in the recording artificial cerebrospinal fluid (aCSF).

2.2. Prenatal ethanol exposure (PAE) protocol in mice

The PAE protocol was adapted with minor modifications from (Kaminen-Ahola et al., 2010b). For the present study, C57Bl/6 male and female mice were mated during the weekend and then separated in different cages. Pregnant mice (n = 8) were exposed to 10 % (v/v) voluntary consumption of EtOH solution during gestation (GD 0–10) (equivalent to the first trimester of pregnancy in humans). Control (CTRL) mice (n = 8) were given water instead of EtOH. Pregnant females were allowed free access to the drinking bottle and food at all times. Mice and drinking tubes were weighed daily to monitor intake. EtOH intake was calculated as grams of 100 % EtOH solution consumed in 24 h/mouse weight (g/kg). (Supplementary fig. 1). Each pregnancy produced approximately 6–7 littermates, which were then divided into subgroups and used for biochemical (protein expression and miRNA dosage), electrophysiological and behavioral experiments.

2.3. Craniofacial dysmorphology

The offspring were analyzed for craniofacial dysmorphic features, to characterize the phenotype of these animals (n = 13 pups randomly selected from 3 different litters). The images were acquired at postnatal day 1 (PND) by a Canon 1100 D model camera, equipped with Canon EF-S 55–250 mm lens + extension tubes (13 + 21 + 31 mm, with high resolution accompanied by graph paper. For each mouse, the following images were acquired: full frontal view (to measure nose width and external and internal eye distance), left or right lateral profile (to measure length and skull width). A total of 5 morphometric measurements were performed for each animal. Facial measurements were achieved by taking reference parameters previously studied for FASD diagnosis in humans (Murawski et al., 2015) and adapted from the work of (Anthony et al., 2010). All 2D images were acquired using a Canon 1100 D camera, equipped with a Canon EF-S 55–250 mm lens + extension tubes (13 + 21 + 31 mm). The analysis of the facial measurements was carried out using an image analysis program (Image-Pro Plus, Media Cybernetics), which allowed us to quantify the morphometric measurements outlined above in the areas of interest. The measurements were expressed in millimeters, through the calibration of the software on graph paper. The individual values obtained from the measurements per animal were then expressed as mean ± SEM and the statistical significance of the differences between the two groups (CTRL, n = 13 and PAE, n = 13) was

evaluated using the Student's unpaired *t*-test (Supplementary fig. 2).

2.4. Growth curve

Offspring were left with their mothers until weaning (at 4 weeks of age) weighed and monitored daily. The growth curve was assessed by measuring body weight expressed in grams. Mice (CTRL = 50 and PAE = 52) were weighed once a week from the first day after birth to PND 28. The values obtained from the weighing of each animal were expressed individually and as mean ± SEM for each point in the timeline (0 PND, 7 PND, 14 PND and 28 PND) (Supplementary fig. 3). The statistical significance of the differences between the two groups (controls, $n = 50$ and PAE, $n = 52$) was assessed using the Mann-Whitney *U* test.

2.5. Preparation of midbrain slices and electrophysiological recordings

Control ($n = 8$) and PAE (n = 8) mice (30 PND) were anesthetized with isoflurane and decapitated for brain collection. Midbrain horizontal slices (250 μm) containing the hippocampi were cut with a vibroslicer (Leica VT1000S, Leica Microsystem, Wetzlar, Germany) in a slicing solution composed of (in mM): NMDG (92), HEPES (20), glucose (25), NaHCO3 (30), NaH2PO4 (1.25), KCl (2.5), MgSO4 (10), CaCl2 (0.5). The solution was ice-cold and carbo-oxygenated with a 95 % O2 + 5 % CO2 gas mixture. Slices were allowed to recover in a low-calcium aCSF solution, composed of (in mM): NaCl (130), KCl (3.5), NaH2PO4 (1.25), NaHCO3 (25), glucose (10), CaCl2 (1) and MgSO4 (2), at 34–35 °C with constant oxygenation for about 1 h before the experiment. Slices were individually transferred to the recording chamber of the patch clamp set up and continuously perfused with warm (32–33 °C), carbo-oxygenated aCSF solution, composed of (in mM): NaCl (130), KCl (3.5), NaH2PO4 (1.25), NaHCO3 (25), glucose (10), CaCl2 (2) and MgSO4 (1). Patch pipettes were made from thin-walled borosilicate capillaries (Harvard Apparatus, London, UK) with a vertical puller (Narishige PP830, Narishige International Ltd., London, UK) back-filled with the following intracellular solution (in mM): K+ Gluconate (120), KCl (15), HEPES (10), EGTA (0.1), MgCl2 (2), Na2PhosphoCreatine (5), Na 2GTP (0.3) and MgATP (2), resulting in a bath resistance of 3–5 MΩ for the recording of spontaneous excitatory postsynaptic currents (sEPSCs). Signals were sampled at 10 kHz and low-pass filtered at 3 kHz with an Axon Multiclamp 700B (Molecular Devices, Sunnyvale, CA, USA). The slice was visualized with an inverted microscope (Nikon Eclipse E600FN) equipped for infrared video-microscopy. All data were analyzed using pCLAMP (Axon Instruments) and GraphPad Software (San Diego, CA). The NMDA receptor blocker AP5 (10 μM) and the GABA blocker gabazine (10 μM) were added to the external solution to isolate sEPSCs AMPAergic currents. Moreover, the passive properties of CA1 neurons were evaluated in CTRL and PAE hippocampi by measuring membrane capacitance, membrane resistance, and resting membrane potential. Finally, to study the effects on the whole intrinsic excitability, increasing steps of depolarizing current (from −10 pA to 210 pA, Δ 20 pA, 500 msec stimulus) were imposed in current-clamp configuration to CA1 neurons to measure the number and threshold of evoked action potentials (APs).

2.6. Real-time PCR (qPCR) for miR-501-3p expression

miRNA from hippocampi were extracted as previously described in (Gerace et al., 2023). Total RNA was isolated from mice hippocampi (CTRL = 9 and PAE = 9) using the TRIzol Reagent (Invitrogen) according to the manufacturer's instructions. RNA was quantified by using the NanoPhotometer® (Implen, Munich, Germany) measuring the absorbance at 260 nm. cDNA was synthesized using the miRCURY LNA RT kit (Qiagen, Hilden, Germany). cDNA samples were stored at −20 °C. RT-quantitative PCR (qPCR) was performed using miRCURY LNA SYBR Green PCR kit (Qiagen) according to the manufacturer's instructions. The following primers from miRCURY LNA miRNA PCR Assays were used: (mir-501-3p: GeneGlobe ID - YP00205037, Quiagen; RNU6b: GeneGlobe ID - YP00203907, Qiagen). The analyses were performed using the Rotor-Gene Q thermal cycler (Qiagen). Each sample was tested in triplicate. RNU6b was selected as reference due to its stability across samples. The calculation of relative expressions was performed using the $2 - \Delta\Delta Ct$ formula.

2.7. Preparation of protein extracts and western blot analyses

Another batch of mice (CTRL = 6 and PAE = 6), exposed to the same protocol described in 2.2, was used for molecular analysis and animals rapidly decapitated at PND30. Proteins from hippocampi were extracted as previously described with minor modifications (Caffino et al., 2018; Gerace et al., 2023, Gerace et al., 2021). Briefly, mice hippocampi were homogenized in a teflon-glass homogenizer in cold 0.32 M sucrose buffer pH 7.4 containing 1 mM HEPES, 1 mM MgCl2, 1 mM NaHCO3 and 0.1 mM PMSF, in presence of commercial cocktails of protease (Roche) and phosphatase (Sigma-Aldrich) inhibitors and an aliquot of each homogenate was then sonicated. The remaining homogenate was centrifuged at 13,000*g* for 15 min obtaining a pellet. This pellet was resuspended in a buffer containing 75 mM KCl and 1 % Triton X-100 and centrifuged at 100,000*g* for 1 h. The resulting pellet, referred as post-synaptic density (PSD) or Triton X-100 insoluble fraction (TIF), was homogenized in a glass–glass potter in 20 mM HEPES, protease and phosphatase inhibitors and stored at −20 °C in presence of glycerol 30 %. Total proteins have been measured in the total homogenate and in the TIF fraction according to the Bradford Protein Assay procedure (Bio-Rad Laboratories, Italy), using bovine serum albumin as calibration standard. Equal amounts of proteins of the homogenate (6 μg) and of TIF fraction (5 μg) were run on criterion TGX precast gels (Bio-Rad Laboratories) under reducing conditions and electrophoretically transferred onto nitrocellulose membrane (Bio-Rad Laboratories). The entire nitrocellulose blot was cut close to the molecular weight at which protein bands are expected to be detected, as indicated by their specific molecular weight and the information depicted in the antibody datasheet. Blots were blocked 1 h at room temperature with I-Block solution (catalogue number: # T2015, Life Technologies, Italia, Italy) in TBS + 0.1 % Tween-20 buffer and incubated with antibodies against the proteins of interest. The conditions of the primary antibodies were the following: anti mGluR5 (1:1000, Millipore, RRID: AB_2295173); anti GRIP (1:2000, Synaptic System, RRID: AB_10804287); anti GluA1 (1:1000, Cell Signaling Technologies, RRID: AB_2732897); anti phospho-GluA1 S831 (1:1000, Cell Signaling Technologies, RRID: AB_2113594); anti GluA2 (1:1000, Cell Signaling Technologies, RRID: AB_10622024); anti GluA3 (1:1000, Merck Millipore, RRID: AB_2113897); anti SAP97 (catalogue number: #ab2057181:1000; Abcam); anti Rab5 (1:1000, Cell Signaling Technologies, RRID: AB_832625); anti Rab11 (1:1000, Cell Signaling Technologies, RRID: AB_10693925); anti vGluT1 (1:1000, Cell Signaling Technologies, RRID: AB_2732897); anti GLT1 (1:1000, Merck Millipore, RRID: AB_941782); anti xCT (1:1000, Abcam, RRID: AB_943744) and anti β-Actin (1:10.000, Sigma, RRID: AB_477593). Results were standardized using β-actin as the control protein, which was detected by evaluating the band density at 43 kDa. Immunocomplexes were visualized by chemiluminescence using the Chemidoc MP Imaging System (RRID: SCR_019037, BioRad Laboratories) and analyzed using the Image Lab software (Bio-Rad Laboratories). Gels were run three times each, and the results represent the average from two different runs. A correction factor was used to average different gels: correction factor gel B = average of (OD protein of interest/OD b-actin for each sample loaded in gel A)/(OD protein of interest/OD β-actin for the same sample loaded in gel B); correction factor gel C = average of (OD protein of interest/OD b-actin for each sample loaded in gel A)/(OD protein of interest/OD b-actin for the same sample loaded in gel C) (Caffino et al., 2018). Full-size original cropped immunoblots related to the protein expression levels evaluated in the study are presented in supplementary fig. 5 and representative

immunoblots for each protein are shown in Figs. 5, 6, 7.

2.8. Behavioral tests

2.8.1. Novel Object recognition test

This paradigm was performed as previously reported (Costa et al., 2022; Provensi et al., 2016; Rani et al., 2021). Briefly, the novel object recognition (NOR) test consisted of 10 min habituation (T0) to the empty arena (45 × 45 × 50 cm), in which the animals familiarized with the test environment. The day after, the mice were placed in the same arena containing two identical plastic objects (cubes or pyramids) for 5 min (training session; T1) followed by a 5 min test session (T2) performed 1 h later, during which one of the familiar objects was replaced by a novel one. The position of the familiar and novel objects (left/right) was randomized to prevent biases. Exploration was defined as sniffing or touching the objects with the nose and/or forepaws. Sitting on or turning around the objects was not considered exploratory behavior. To analyze recognition memory, the exploration time (%) was calculated as: [Time exploring the novel object (s) X 100 / total time of objects exploration (s)]. The discrimination index (DI) is calculated as follows: [(Time spent Novel Object:Total exploration time)-(Time spent Familiar Object:Total exploration time) X 100]. Control animals are expected to spend more time exploring the novel object than the familiar one, as index of intact short-term memory. Mice behavior was filmed and videos analyzed by an experienced observer unaware of the treatments.

2.8.2. Open field

This paradigm was performed as previously reported in (Costa et al., 2022; Rani et al., 2021). Mice locomotor activity and anxiety-like level were tested in an open arena (45 × 45 × 50 cm) where a virtual zone (20 × 20 cm) was delimited in the center of the arena. Mice were allowed to freely explore the arena for 10 min. In between observations, the arena was cleaned with 30 % ethyl alcohol in water to remove possible scent cues left by the animal. Time spent and number of entries at the center and periphery of the open field and total distance travelled were measured and analyzed using the video tracking system Any-maze software (Any-Maze v7.15).

2.8.3. Sucrose preference test

Another batch of mice (CTRL = 13 and PAE = 9), exposed to the same protocol described in 2.2, was used for Sucrose preference test. The experimental paradigm was performed as previously reported in (Ilari et al., 2022). Mice were individually housed in single cages with continuous access to water for the first 2 days (habituation) and with continuous access to water and a solution of sucrose at 5 % (*w/v*) for the last 2 days (sucrose preference test). The bottles were weighed and switched every day, to prevent development of side preference. Sucrose preference was calculated as the intake of sucrose solution/total fluid intake (%).

2.9. Statistical analysis

Data are presented as means ± SEM of n experiments from independent animals. Data were analyzed using pCLAMP (Axon Instruments) and Prism 8 software (GraphPad Software, San Diego, CA, USA). The statistical significance of differences between Western blot optical densities, miRNA levels, body weight and craniofacial dysmorphic features was evaluated by performing Student's *t*-test or Mann-Whitney *U* test, as appropriate. For electrophysiological experiments and behavioral analysis, statistical significance was evaluated by performing Student's t-test, or one- or two-way ANOVA followed by Bonferroni post hoc tests for unpaired samples and two-way ANOVA followed by Sidak's post hoc tests for paired samples, as appropriate. Differences were considered significant for $^{*}p < 0.05$, $^{**}p < 0.01$, $^{***}p < 0.001$ and $^{****}p < 0.0001$. All statistical calculations were performed using GRAPH-PAD PRISM v.8 for Windows (GraphPad Software).

3. Results

In the present paper, C57Bl/6 pregnant mice were exposed to 10 % (*v*/v) voluntary EtOH during gestation (GD 0–10) and then, they were exposed to water for the rest of pregnancy (Fig. 1). The average daily consumption of EtOH intake resulted in 12.95 ± 0.91 g of EtOH/kg body weight/day (Supplementary Fig. 1). The offspring were then analyzed for craniofacial dysmorphic features. We observed only a slight reduction of the nose length in PAE mice respect to controls (Fig. 2 and Supplementary Fig. 2). Unexpectedly, no differences were observed in the growth curve (expressed as body weight) between PAE and control mice (Supplementary Fig. 3), indicating that these animals did not display marked physical characteristics.

Significant changes were observed in the functional properties of hippocampal CA1 neurons from PAE adolescent mice compared to controls. Specifically, no differences were observed in the basal parameters, such as membrane capacitance, membrane resistance and resting membrane potentials (Fig. 3, panel A), whereas a decreased number of total action potentials was found (AP) (Fig. 3, panel B and C), which did not affect the threshold (Fig. 3, panel D). In addition, both frequency and amplitude of AMPA sEPSCs were significantly decreased (Fig. 4), indicating a permanent impairment of the AMPAergic circuitry. Accordingly, we found that the expression of miR-501-3p (one of the microRNAs which translationally represses the AMPA subunit GluA1, Fig. 5, panel A), is upregulated in the hippocampi of PAE mice compared to CTRL (Fig. 5, panel B), indicative of defective expression and changes in subunit composition of AMPA channels. This effect was paralleled by increased expression of mGluR5 in PAE mice (Fig. 5, panel C).

Therefore, we analyzed the expression of the main AMPA subunits (GluA1, GluA2 and GluA3) and their specific scaffolding proteins (GRIP and SAP97), which anchor receptors at the membrane, thus allowing physiological neurotransmission, in the total homogenate (Supplementary Table 1) and in the post-synaptic density (PSD). The expression of GluA1, GluA2 and GluA3 AMPAR subunits (Fig. 6, panel A, B and C) and their scaffolding proteins GRIP and SAP97 (Fig. 6, panel G and H) were enhanced in PAE mice compared to controls. In addition, in line with our electrophysiological results showing reduced amplitude of AMPA-isolated sEPSCs (Fig. 4), the phosphorylation (activation) levels of the GluA1 subunit were significantly decreased (Fig. 6, panel D), suggestive of AMPA dysfunction. To further understand whether PAE alters AMPA receptor subunit composition, we measured the GluA1/GluA2 and GluA2/GluA3 ratio in the postsynaptic density. PAE increased the GluA1/GluA2 ratio (Fig. 6, panel E), while no changes were observed in the GluA2/GluA3 ratio (Fig. 6, panel F). To investigate whether PAE-induced increase in AMPA receptor subunits localization in the PSD might involve endocytic mechanisms, we evaluated the expression of molecular determinants of intracellular vesicular trafficking related to AMPA endocytosis, i.e. Rab5, a GTPase required for membrane receptor internalization and early endosome generation, and Rab11, a marker for recycling endosomes (Zerial and McBride, 2001). Interestingly, both Rab5 (Fig. 6, panel I) and Rab11 (Fig. 6, panel L) expression levels were reduced in PAE mice, suggesting that the increased AMPA retention might be due to a PAE-induced alterations in the endocytotic machinery.

Furthermore, examining the expression of the main glutamate transporters (vGluT1, GLT1 and xCT), we found increased levels of both vesicular and astrocytic glutamate transporters, vGluT1 and GLT1, respectively (Fig. 7, panel A and B), thus suggesting that an increased release of glutamate is balanced by an increased reuptake, likely unaffecting glutamate concentration in the synaptic cleft. Conversely, the expression of the cystine/glutamate antiporter xCT, which mediates the uptake of extracellular cystine in exchange for glutamate, was significantly decreased in PAE hippocampi (Fig. 7, panel C), suggestive a reduced release of glutamate at extrasynaptic sites.

To unveil whether the observed molecular alterations might contribute to alter cognitive function, we performed the novel object recognition test, to assess short-term recognition memory in our

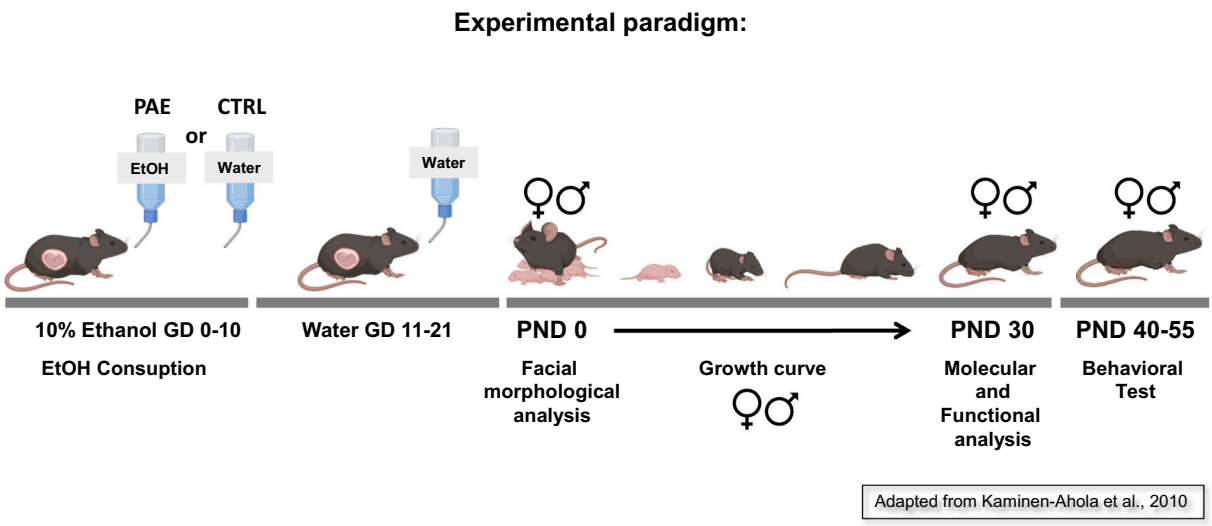

Fig. 1. Experimental protocol showing C57Bl/6 pregnant mice exposed to 10 % EtOH during gestation (GD 0–10; PAE) and then to water for the entire period of pregnancy or to water throughout the entire gestation period (CTRL). The offspring were then analyzed for: craniofacial dysmorphic feature (PND 1), growth curve (PND 0–28), protein expression in postsynaptic compartment and electrical properties from CA1 neurons (PND 28–30) and behavioral test to assess memory and locomotor activity (PND 40–55).

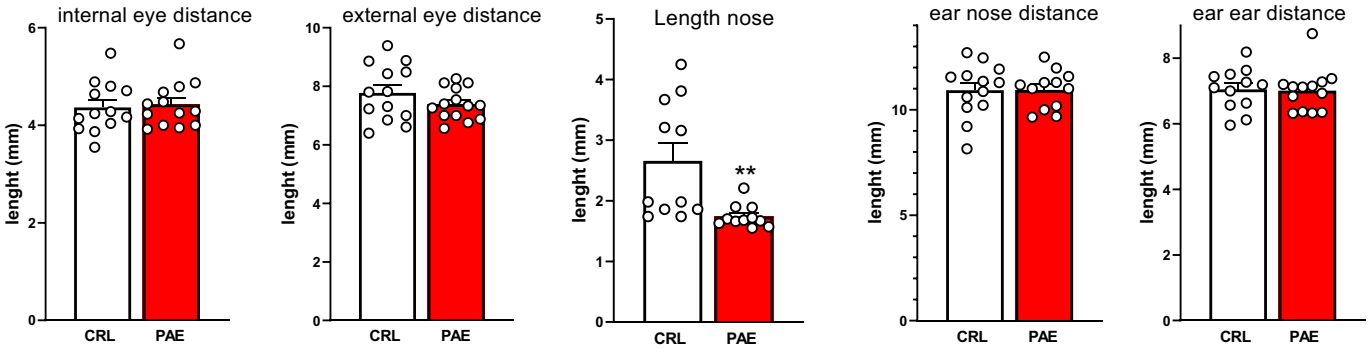

Fig. 2. Craniofacial dysmorphic features in PAE C57Bl/6 mice. The offspring (CTRL; $N = 13$ and PAE; N = 13) were analyzed for craniofacial dysmorphic features at postnatal day 1 (PND). For each experimental mouse were acquired the full frontal view, left or right lateral profile. The measurements were expressed in millimeters, through the calibration of the software (Image-Pro Plus, Media Cybernetics) on graph paper. The individual values obtained from the measurements per animal were expressed as mean ± SEM. A slight reduction of the length nose in PAE C57Bl/6 respect to control mice was observed. No differences in the other parameters evaluated. Statistical significance was evaluated using the Mann-Whitney *U* test. Differences were considered significant at $^{**}p < 0.01$. All statistical calculations were performed using GRAPH-PAD PRISM v.8 for Windows (GraphPad Software).

animals. PAE mice spent less time exploring the novel object than the familiar one compared to control animals, indicating that PAE impaired memory recognition (Fig. 8, panel C). These effects are not due to alterations in general locomotor activity, indeed no differences were observed in the total distance travelled by PAE and control mice during the open field test (Fig. 9, panel B). Moreover, the time spent and the number of entries at the center (Fig. 9, panel E) and periphery zone (Fig. 9, panel D) of the open field arena were not different between the two groups, indicating that our mice did not manifest a significant state of anxiety. Finally, we performed the sucrose preference test and we found no differences in the haedonic tone between the two experimental groups (Supplementary Fig. 4).

4. Discussion

Our findings demonstrate that PAE causes molecular, electrophysiological and cognitive dysfunctions in the hippocampus of adolescent mice, adding a novel piece to the puzzle of the changes set in motion by PAE and corroborating our previous in vitro findings.

We generated an in vivo model of PAE, by exposing C57Bl/6 pregnant mice to 10 % EtOH during gestation (GD 0–10). Under our experimental conditions, the animals do not display a marked phenotype, which is acceptable taking into consideration the wide range of FASD cases. Indeed, facial dysmorphology may not be prominent in FASD individuals and the morphological deficits observed early in life are often no longer recognizable (Wozniak et al., 2019). Specifically, we noted a minor decrease in nose length, with no notable variances in other morphological traits or in growth trajectory between PAE and control mice. However, despite the lack of gross changes, we found that PAE exerted a significant effect on cognition, as witnessed by a significant impairment in recognition memory. In fact, PAE mice spent less time exploring the novel object, indicating impaired recognition memory, an effect that cannot be traced back to alterations in locomotor activity, as evidenced by the open field test. Impaired cognition has been already shown after PAE. In fact, it has been observed an increased escape latency in PAE offspring that persist in older pups (An and Zhang, 2015; Gianoulakis, 1990; Matthews and Simson, 1998) as well as alterations in avoidance learning and the object–place paired-associate

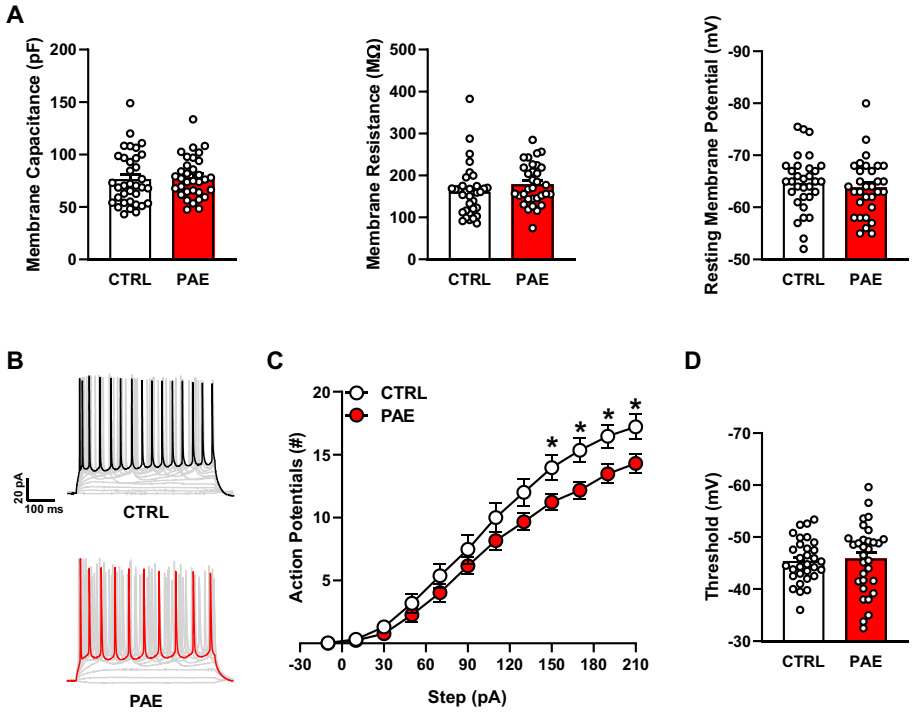

Fig. 3. Passive properties and intrinsic somatic excitability in CA1 neurons from CTRL and PAE mice. A) Bar graph showing no differences in the membrane capacitance, membrane resistance and resting membrane potential (CTRL; $n = 30$, PAE; n = 30) between CTRL ($N = 8$) and PAE (N = 8) mice. B) Representative example traces of whole-cell current clamp action potentials (APs) recorded from CA1 pyramidal cells (CTRL; n = 30, PAE; n = 30) evoked by increasing depolarizing step (20 pA), in control and PAE mice. C) Mean number of spikes plotted against current input amplitude showing the decrease of the total AP number in CA1 neurons from PAE mice (red circles) compared to controls (black circles). Bars represent the mean ± SEM, $*p < 0.05$, (unpaired *t*-test). D) Bar chart showing no differences in the threshold values (mV) between the two experimental groups. (For interpretation of the references to colour in this figure legend, the reader is referred to the web version of this article.)

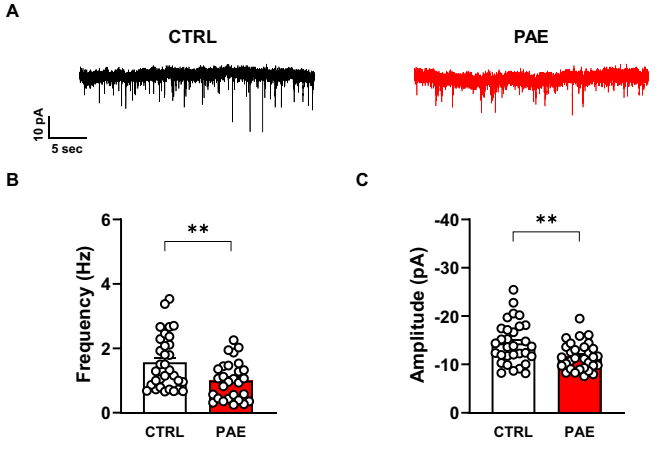

Fig. 4. Spontaneous AMPA excitatory postsynaptic currents (sEPSCs) in CA1 pyramidal cells in CTRL and PAE mice A) Representative traces of results obtained in independent neurons (CTRL; n = 30, PAE; n = 30) from CTRL (N = 8) and PAE (N = 8) for each condition. (B—C) Bar chart of quantitative data expressed as CTRL frequency (Hz) (Panel B) and amplitude (pA) (Panel C) showing that PAE significantly decreases both frequency and amplitude of AMPA-sEPSCs. Bars represent the mean ± SEM, **p < 0.01; $*p < 0.1$ vs CRL (unpaired t-test).

task in rats (Mira et al., 2020; Sanchez et al., 2019). Furthermore, it has been shown that mice exposed to EtOH are predisposed to exhibit traits of anxiety and depression in adulthood (Abbott et al., 2016; Hellemans et al., 2010). Nevertheless, our PAE mice showed neither anxiety nor depression-like symptoms. However, we must consider that the open field test is not the best for measuring anxiety and that the sucrose test only reflects the more strictly hedonic aspect of depression and not other characteristic traits of this disease.

We found significant changes in the functional properties of hippocampal CA1 neurons from PAE adolescent mice compared to controls. Specifically, we found a decreased number of the total AP, indicating a reduced neuronal excitability. Furthermore, examining the excitatory responses particularly focusing on AMPARs, whose activity is associated to learning and memory, we observed a significant reduction of both frequency and amplitude of AMPA sEPSCs in CA1 neurons, suggesting that PAE elicits a long-term impairment of the AMPAergic circuitry. Notably, these data confirm our previous in vitro results. In fact, immature organotypic hippocampal slice chronically exposed to EtOH during maturation display a significant reduction in either frequency or amplitude of AMPA-mediated synaptic transmission (Gerace et al., 2023). The present data support that EtOH-induced repression of AMPA transmission is a long-lasting mechanism that is present and maintained in PAE litters. In addition, also the up-regulation of miR-501-3p in the hippocampus of PAE adolescent mice confirms our previous in vitro results (Gerace et al., 2023) pointing to the levels of miR-501-3p as a critical, long-term mechanism of PAE.

It is important to note that both electrophysiological and miRNA data are suggestive of defective expression and changes in the subunit composition of AMPA channels. Opposite to the EtOH-induced reduction in the AMPA subunits observed in vitro, in vivo we found increased expression of AMPAR subunits in PAE hippocampi compared to controls, an effect similarly observed by other authors in comparable experimental conditions (Dettmer et al., 2003; Takahashi et al., 2021). In detail, increased GluA2 density was observed in cerebral cortex of guinea pigs exposed to alcohol during gestation (Dettmer et al., 2003) and alcohol enhanced AMPAR subunits in the dentate gyrus of adult rats

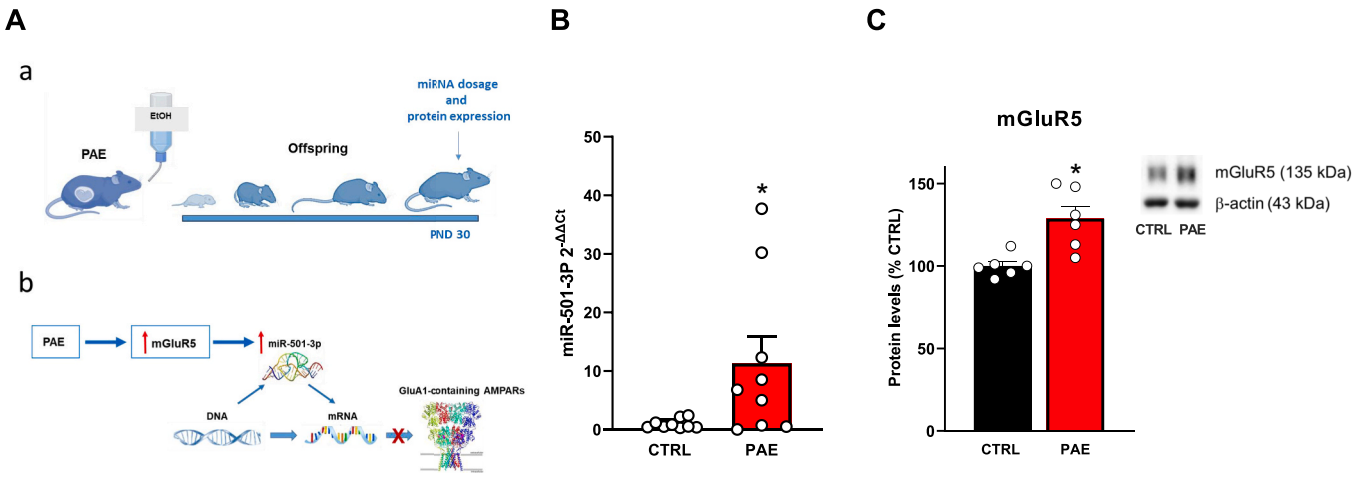

Fig. 5. PAE-induced upregulation of miR-501-3p and mGluR5 protein expression in the hippocampus. (A) Graphical scheme representing a) the experimental timeline and b) the regulation of miR-501-3p induced by PAE in offspring. B) Real-time PCR was performed to assess miR-501-3p expression in the hippocampus of CTRL and PAE mice. Data are expressed as $2 - \Delta\Delta Ct$. Bars represent the mean ± SEM of 9 hippocampi from independent mice. (Data are expressed as percentage of CTRL protein levels (white column). (C) mGluR5 protein expression was measured in the homogenate of PAE ($N = 6$) and CTRL ($N = 6$) hippocampi. Bars represent the mean ± SEM of six hippocampi from independent mice. *$p < 0.05$ versus CTRL (Mann-Whitney U test).

(Takahashi et al., 2021). These molecular alterations were correlated to attention (Louth et al., 2016) and cognitive (Vaglenova et al., 2008) deficits in offspring. Thus, we may suggest that such persistent increase in the expression of the main AMPA receptor subunits may result in exaggerated strengthening of synapses, thus overriding the physiological functioning of synaptic networks, leading to less plastic synapses and, ultimately, to impaired response in a cognitive-demanding test such as NOR.

Moreover, our electrophysiological and miRNA data are corroborated by the reduced phosphorylation of the major AMPAR subunit GluA1. Notably, such reduction occurs despite the enhanced total levels of this subunit, strongly suggesting its inactivation. It is important to note that also the GluA2 and GluA3 AMPA subunits were significantly upregulated, suggesting an overall, long-lasting effect of PAE. Interestingly, when measuring the ratio GluA1/GluA2, we found an increase that may be indicative of a PAE-induced reorganization of AMPAR subunit composition; in fact, such effect may suggest a more excitable synaptic network since GluA1/GluA2 containing AMPA receptors move into the PSD as a consequence of synaptic plasticity to sustain neuronal activity (Shi et al., 2001). In addition, the increased ratio suggests that PAE has induced a switch toward GluA2-lacking AMPA receptors, in line with the strengthening of the synapses above mentioned. This is further substantiated by the evidence that the increased expression of AMPA receptors in the PSD is accompanied by an increased expression of their main scaffolding proteins GRIP and SAP97. This indicates that these receptors are tightly retained at the membrane thus preventing the normal shuttling between synaptic and extra-synaptic sites. Another piece of information in line with this interpretation derives from the evidence that PAE alters the mechanisms subserving endosomal sorting. In fact, the reduced expression of Rab5, a marker of early endosome that regulate AMPAR endocytosis (Bucci et al., 1992; Hausser and Schlett, 2019) and Rab11, a key regulator of AMPAR recycling to the membrane surface to facilitate synaptic plasticity (Brown et al., 2007), further strengthen the possibility that the reduced AMPAR expression is primarily due to AMPAR internalization in the hippocampus of PAE mice, thus contributing to alter hippocampal synaptic properties.

The investigation of the effects of PAE on presynaptic glutamate mechanisms suggests an increase of glutamate evoked by increased levels of vGluT1; interestingly, this might be buffered by the increased reuptake into astrocytes mediated by the increased GLT1. This is important since we found increased expression of mGluR5 receptors, which are primarily expressed at extra-synaptic sites and astrocyte (Luján et al., 1996). Since mGluR5 positively regulates the expression of GLT1 (Vermeiren et al., 2005), it is tempted to speculate that PAE-induced expression of mGluR5 is a defensive strategy to counteract the increased glutamate release, as evidenced by vGluT1 up-regulation. This balance in glutamate homeostasis is further supported by the reduced expression of the Cystine/glutamate antiporter xCT^- contributing to lowering glutamate spillover at extra-synaptic sites (Bridges et al., 2012), thus preventing its excitotoxic activity.

In summary, our findings demonstrate that PAE causes a general dysregulation of the AMPAergic synapse, resulting in the formation of less functional AMPAergic synapses. The synaptic changes observed in our PAE model could represent an aberrant form of synaptic plasticity that may underlie hippocampal-dependent memory deficit. While our study integrates molecular, functional, and behavioral analyses, it also has some limitations. Although our experimental paradigms partially mimic the effects observed in children with PAE, exhibiting minimal physical changes but significant neurobiological alterations, it is worth noting that, in the present protocol, EtOH exposure in pregnant mice is voluntary, albeit restricted to a single bottle choice. Furthermore, we chose not to segregate males and females, as we did not detect notable functional or behavioral gender disparities. Additionally, despite we demonstrated in vitro a direct relationship between miRNA 501-3p and AMPARs, we cannot infer the same conclusion from this study; in fact, we lack the ability to elucidate the precise connection between the upregulated miR501-3p and the ineffective suppression of GluA1. We can hypothesize that PAE induces heightened expression of hippocampal miR-501-3p during the fetal stage, thereby constraining GluA1 expression and proper AMPA neurotransmission in the early phases of life. Consequently, in an effort to rebalance the excitatory/inhibitory transmission, AMPAR subunits become overexpressed via reduced activity of the endocytic machinery; however, these newly formed AMPARs, an effect that persists at least until adolescence, exhibit dysfunctional properties that may contribute to alter synaptic plasticity, thus modifying the maturational trajectory of the brain and consequently impairing behavioral outputs. Further research is required to identify the temporal window of miR-501-3p to fully understand this intricate mechanism.

Overall, our findings provide valuable insights into the mechanisms induced by PAE and their associations with molecular, functional, and memory processes. These insights are crucial for understanding the long-term effects of PAE, including cognitive deficits, psychiatric disorders, and susceptibility to alcohol addiction in adulthood. Our results

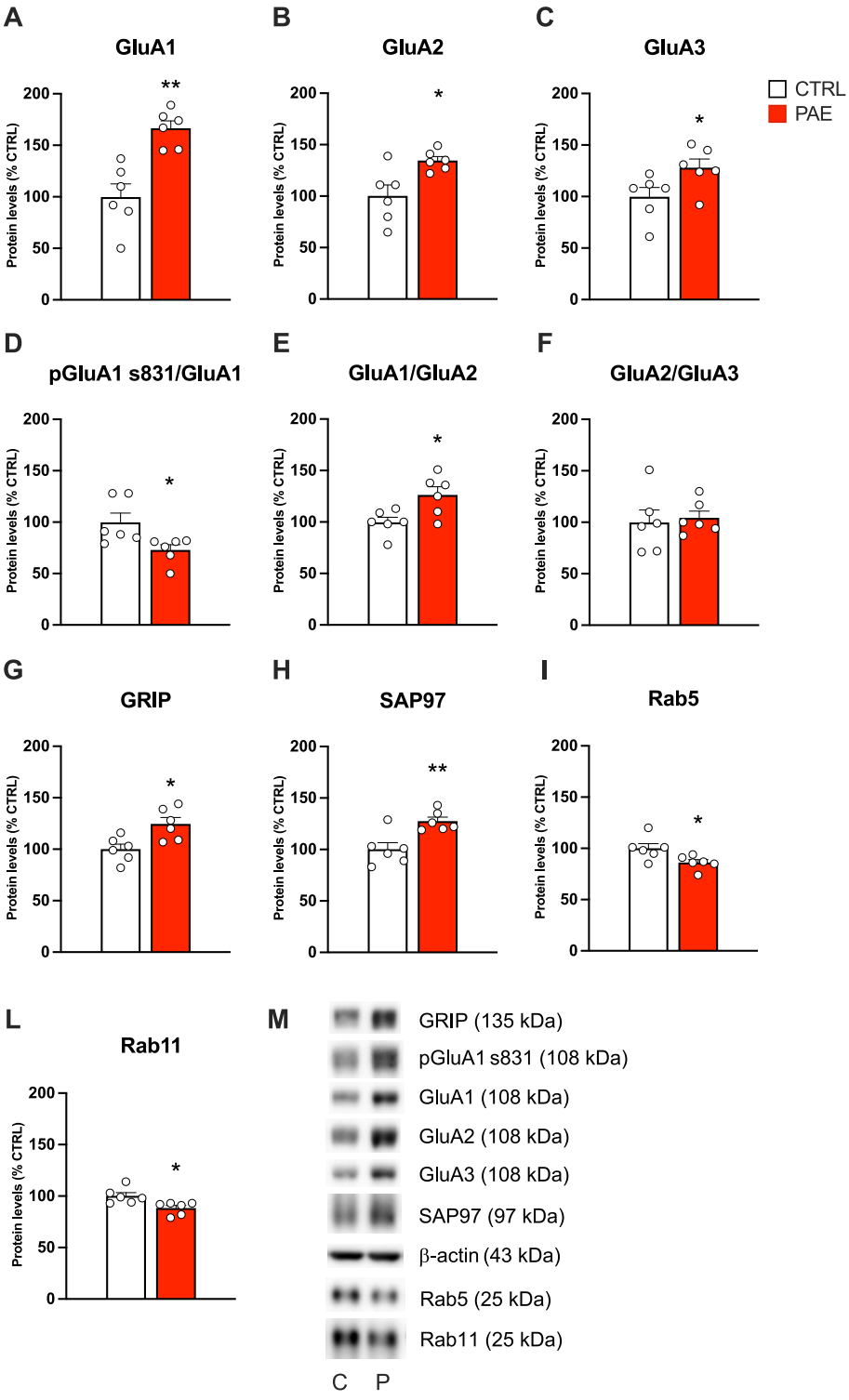

Fig. 6. PAE alters the expression of AMPA subunits and related scaffolding proteins in the Post Synaptic Density (PSD) and of endosomal markers in the homogenate of the hippocampus. Experiments were conducted as described in Fig. 1. The main AMPA receptor subunits GluA1 (A), GluA2 (B) and GluA3 (C) and their specific scaffolding proteins glutamate receptor-interacting protein (GRIP; G) and synapse-associated protein 97 (SAP97; H) are significantly increased in the hippocampal PSD of PAE mice respect to CTRL. The GluA1 phosphorylation levels (D) were significantly decreased in PAE hippocampi versus CTRL. The ratio GluA1/GluA2 (E) but not GluA2/GluA3 (F) is significantly increased in PAE mice. Rab5 (I) and Rab11 (L) expression, markers of early and of recycling endosome respectively, was significantly reduced in the homogenate of PAE hippocampi. (M) Representative immunoblots of the proteins of interest are shown in the lower panel. Data are expressed as percentage of CTRL protein levels (white column). Bars represent the mean ± SEM of six hippocampi from independent mice $^{**}p < 0.01$ and $^{*}p < 0.05$ versus CTRL (Mann-Whitney U test).

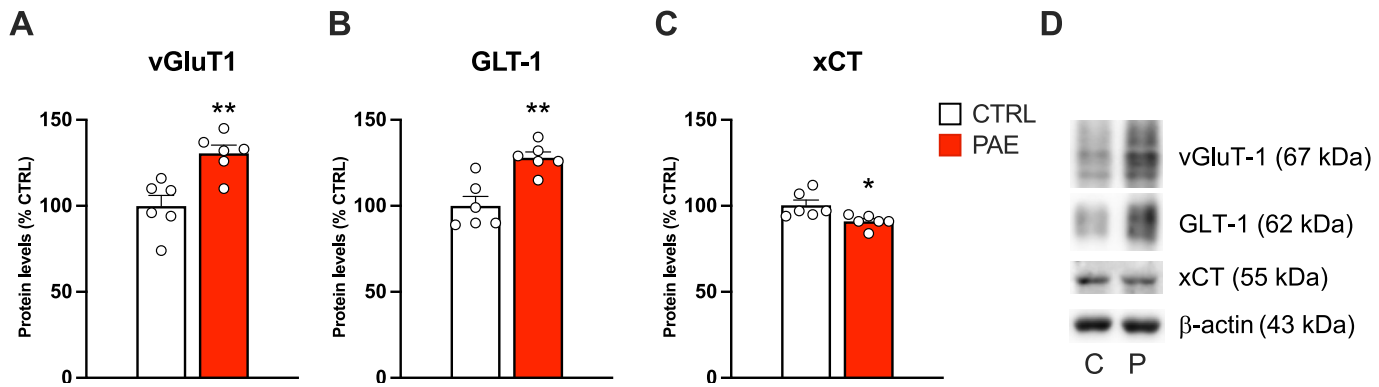

Fig. 7. PAE alters the expression of glutamate transporters in the homogenate of the hippocampus. The experiments were conducted as described in Fig. 1. The glutamate transporters vGluT1 (A) and GLT1 (B) are significantly increased in PAE mice respect to CTRL, while xCT protein was significantly decreased (C). (D) Representative immunoblots of the proteins of interest. Data are expressed as percentage of CTRL protein levels (white column). Bars represent the mean ± SEM of six hippocampi from independent mice $^{**}p < 0.01$ and $^{*}p < 0.05$ versus CTRL (Mann-Whitney U test).

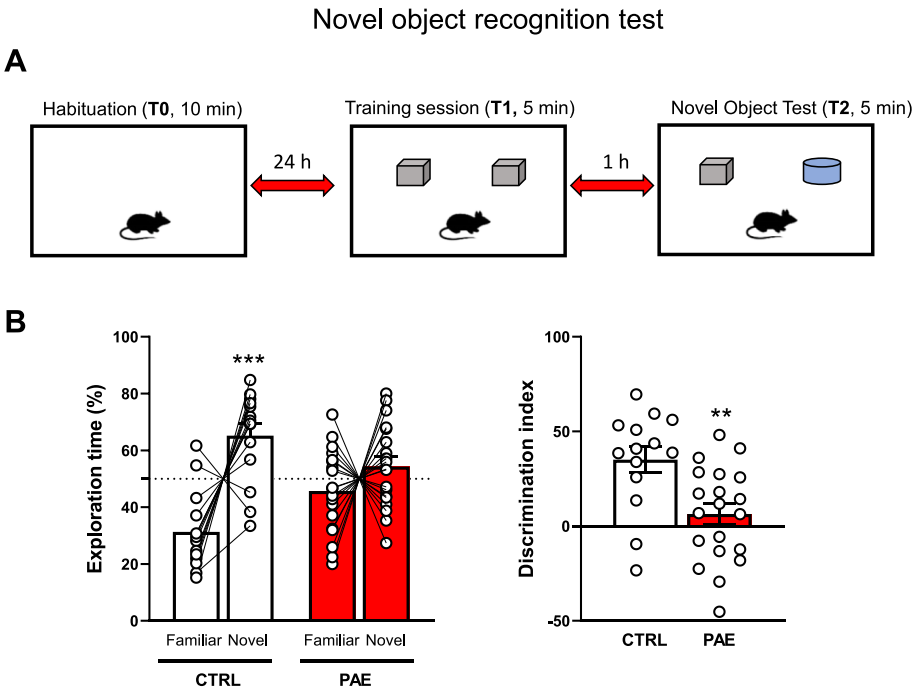

Fig. 8. PAE-induced cognitive impairment in the novel object recognition test. (A) Experimental protocol showing C57Bl/6 PAE mice exposed for 5 min in an empty arena (habituation; T0), the day after, the mice were placed in the same arena in presence of two identical plastic objects (training session; T1) followed by a test session (novel object test; T2) performed 1 h later in the presence of one familiar and a novel object. (B) Bar graphs represent the scatter plot of the exploration time (left panel) and the discrimination index (right panel) showing that PAE mice ($N = 20$) show memory impairment respect to CTRL ($N = 14$). $^{***}p < 0.001$; $^{**}p < 0.01$; vs. familiar object (two-way ANOVA followed by Bonferroni test and Mann-Whitney U test).

underscore the importance of addressing PAE as it significantly increases the risk of psychiatric conditions, such as harmful alcohol use and psychostimulant addiction, in adolescents and adults (Wang et al., 2019; Duko et al., 2020).

Funding and disclosures

This research was supported by grants from MUR PRIN2022X9X5MS (to GM and MU), MUR PRIN 2022CZTZ87 (to LC), MUR PRIN P2022E4MLS (to LC and NC), MUR PRIN 20227HRFPJ (to FF), MUR PRIN PNRR P202274WPN (to FF) and by grants from MIUR Progetto Eccellenza 2023/2027.

Ethical Statement

All procedures performed in this study involving animals were conducted according to the European Community guidelines for animal care (Directive 2010/63/EU). The study protocol was approved by the Committee for Animal Care and Experimental Use of the University of Florence and authorized by the Italian Ministry of Health (Authorization number 545/2018). The authors further attest that all efforts were made to minimize the number of animals used and their suffering.

CRediT authorship contribution statement

Lorenzo Curti: Writing – review & editing, Methodology, Investigation, Formal analysis, Data curation. **Beatrice Rizzi:** Methodology,

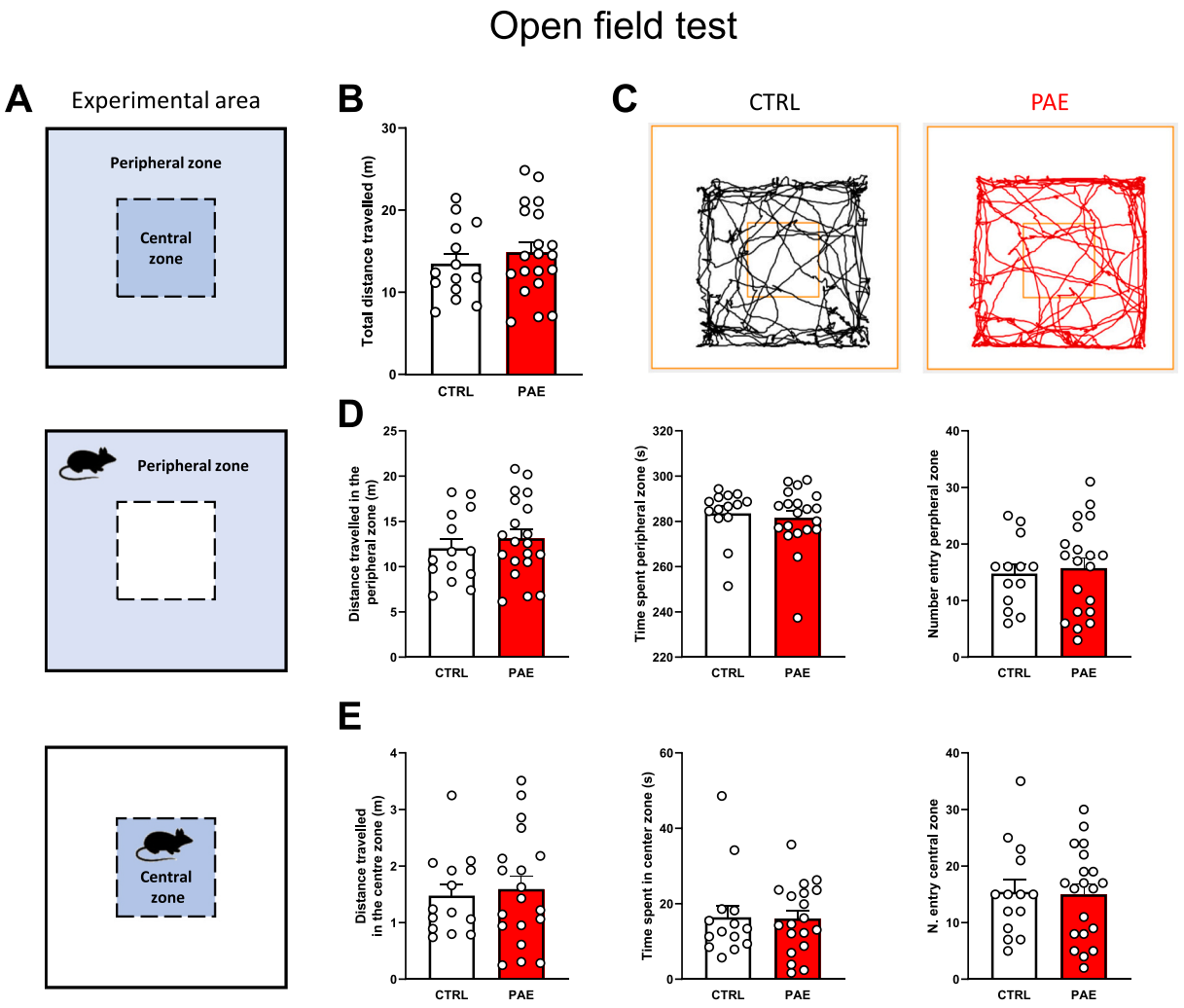

Fig. 9. Open field test in PAE and CTRL mice. (A) Experimental area showing the open arena in which was delimited a central virtual zone in which PAE and CTRL mice were allowed to freely explore for 10 min to test locomotor activity and anxiety-related behavior. (C) Representative track plot reports recorded during the 10 min test sessions. Bars represent total distance travelled (B), time spent and number of entries at the center (E) and periphery (D) of the open field arena analyzed using the video tracking system Any-maze software (Any-Maze v7.15). No differences were recorded in both locomotor activity and anxiety-related behavior between the PAE (N = 20) and CTRL (N = 14) mice.

Investigation, Formal analysis, Data curation. **Francesca Mottarlini:** Methodology, Investigation, Formal analysis, Data curation. **Alice Ilari:** Methodology, Investigation, Conceptualization. **Virginia Sordi:** Methodology, Formal analysis. **Giuseppe Ranieri:** Methodology. **Cristina Luceri:** Validation, Methodology, Investigation, Data curation. **Nazzareno Cannella:** Writing – review & editing, Validation, Conceptualization. **Massimo Ubaldi:** Validation, Supervision, Project administration, Funding acquisition. **Alessio Masi:** Methodology, Investigation, Formal analysis. **Fabio Fumagalli:** Writing – review & editing, Validation, Supervision, Resources, Funding acquisition, Conceptualization. **Lucia Caffino:** Writing – review & editing, Validation, Supervision, Investigation, Funding acquisition, Data curation, Conceptualization. **Guido Mannaioni:** Writing – review & editing, Validation, Supervision, Resources, Project administration, Funding acquisition. **Elisabetta Gerace:** Writing – review & editing, Methodology, Formal analysis, Data curation.

Declaration of competing interest

The authors declare that they have no known competing financial interests or personal relationships that could have appeared to influence the work reported in this paper.

Data availability

Data will be made available on request.

Acknowledgements

Francesca Mottarlini is recipient of a post-doctoral fellow funded by Zardi-Gori foundation. Beatrice Rizzi is supported by cycle XXXVIII of the PhD programme in Theoretical and Applied Neuroscience, DM351 (Finanziamenti PNRR).

Appendix A. Supplementary data

Supplementary data to this article can be found online at https://doi.org/10.1016/j.pnpbp.2024.111174.

References

Abbott, C.W., Kozanian, O.O., Kanaan, J., Wendel, K.M., Huffman, K.J., 2016. The impact of prenatal ethanol exposure on neuroanatomical and behavioral development in mice. Alcohol. Clin. Exp. Res. 40, 122–133. https://doi.org/10.1111/ACER.12936.

An, L., Zhang, T., 2015. Prenatal ethanol exposure impairs spatial cognition and synaptic plasticity in female rats. Alcohol 49, 581–588. https://doi.org/10.1016/J.ALCOHOL.2015.05.004.

Anifandis, G., Bounartzi, T., Messini, C.I., Dafopoulos, K., Sotiriou, S., Messinis, I.E., 2014. The impact of cigarette smoking and alcohol consumption on sperm parameters and sperm DNA fragmentation (SDF) measured by Halosperm®. Arch. Gynecol. Obstet. 2014 (290), 777–782. https://doi.org/10.1007/s00404-014-3281-x.

Anthony, E.K., Austin, M.J., Cormier, D.R., 2010. Early detection of prenatal substance exposure and the role of child welfare. Child Youth Serv. Rev. 32, 6–12. https://doi.org/10.1016/j.childyouth.2009.06.006.

Balaraman, S., Tingling, J.D., Tsai, P., Miranda, R.C., 2013. 2013. Dysregulation of microRNA expression and function contributes to the etiology of fetal alcohol Spectrum disorders. Alcohol Res. 35 (1), 18–24.

Bellinger, F.P., Davidson, M.S., Bedi, K.S., Wilce, P.A., 2002. Neonatal ethanol exposure reduces AMPA but not NMDA receptor levels in the rat neocortex. Dev. Brain Res. 136, 77–84. https://doi.org/10.1016/S0165-3806(02)00363-2.

Bower, E., Szajer, J., Mattson, S.N., Riley, E.P., Murphy, C., 2013. Impaired odor identification in children with histories of heavy prenatal alcohol exposure. Alcohol 47, 275–278. https://doi.org/10.1016/j.alcohol.2013.03.002.

Bridges, R., Lutgen, V., Lobner, D., Baker, D.A., 2012. Thinking outside the cleft to understand synaptic activity: contribution of the cystine-glutamate antiporter (system xc-) to normal and pathological glutamatergic signaling. Pharmacol. Rev. 64, 780–802. https://doi.org/10.1124/pr.110.003889.

Brown, T.C., Correia, S.S., Petrok, C.N., Esteban, J.A., 2007. Functional compartmentalization of endosomal trafficking for the synaptic delivery of AMPA receptors during long-term potentiation. J. Neurosci. 27, 13311–13315. https://doi.org/10.1523/JNEUROSCI.4258-07.2007.

Bucci, C., Parton, R.G., Mather, I.H., Stunnenberg, H., Simons, K., Hoflack, B., Zerial, M., 1992. The small GTPase rab5 functions as a regulatory factor in the early endocytic pathway. Cell 70, 715–728. https://doi.org/10.1016/0092-8674(92)90306-W.

Caffino, L., Messa, G., Fumagalli, F., 2018. A single cocaine administration alters dendritic spine morphology and impairs glutamate receptor synaptic retention in the medial prefrontal cortex of adolescent rats. Neuropharmacology 140, 209–216. https://doi.org/10.1016/j.neuropharm.2018.08.006.

Cantacorps, L., Alfonso-Loeches, S., Guerri, C., Valverde, O., 2019. Long-term epigenetic changes in offspring mice exposed to alcohol during gestation and lactation. J. Psychopharmacol. 33, 1562–1572. https://doi.org/10.1177/0269881119856001.

Charness, M.E., Riley, E.P., Sowell, E.R., 2016. Drinking during pregnancy and the developing brain: is any amount safe? Trends Cogn. Sci. https://doi.org/10.1016/j.tics.2015.09.011.

Costa, A., Rani, B., Bastiaanssen, T.F.S., Bonfiglio, F., Gunnigle, E., Provensi, G., Rossitto, M., Böhme, M., Strain, C., Martínez, C.S., Blandina, P., Cryan, J.F., Layé, S., Corradetti, R., Passani, M.B., 2022. Diet prevents social stress-induced maladaptive Neurobehavioural and gut microbiota changes in a histamine-dependent manner. Int. J. Mol. Sci. 23. https://doi.org/10.3390/ijms23020862.

Darbinian, N., Darbinyan, A., Merabova, N., Bajwa, A., Tatevosian, G., Martirosyan, D., Zhao, H., Selzer, M.E., Goetzl, L., 2021. Ethanol-mediated alterations in oligodendrocyte differentiation in the developing brain. Neurobiol. Dis. 148, 105181. https://doi.org/10.1016/j.nbd.2020.105181.

Dettmer, T.S., Barnes, A., Iqbal, U., Bailey, C.D.C., Reynolds, J.N., Brien, J.F., Valenzuela, C.F., 2003. Chronic prenatal ethanol exposure alters ionotropic glutamate receptor subunit protein levels in the adult guinea pig cerebral cortex. Alcohol. Clin. Exp. Res. 27, 677–681. https://doi.org/10.1097/01.ALC.0000060521.32215.E9.

Gerace, E., Landucci, E., Totti, A., Bani, D., Guasti, D., Baronti, R., Moroni, F., Mannaioni, G., Pellegrini-Giampietro, D.E., 2016. Ethanol toxicity during brain development: alterations of excitatory synaptic transmission in immature Organotypic hippocampal slice cultures. Alcohol. Clin. Exp. Res. 40, 706–716. https://doi.org/10.1111/acer.13006.

Gerace, E., Ilari, A., Caffino, L., Buonvicino, D., Lana, D., Ugolini, F., Resta, F., Nosi, D., Grazia Giovannini, M., Ciccocioppo, R., Fumagalli, F., Pellegrini-Giampietro, D.E., Masi, A., Mannaioni, G., 2021. Ethanol neurotoxicity is mediated by changes in expression, surface localization and functional properties of glutamate AMPA receptors. J. Neurochem. 157, 2106–2118. https://doi.org/10.1111/jnc.15223.

Duko, B., Pereira, G., Betts, K., Tait, R.J., Newnham, J., Alati, R., 2020. Associations of prenatal alcohol exposure and offspring harmful alcohol use: findings from the Raine Study. Drug Alcohol Depend. https://doi.org/10.1016/j.drugalcdep.2020.108305.

Gerace, E., Curti, L., Caffino, L., Bigagli, E., Mottarlini, F., Castillo Díaz, F., Ilari, A., Luceri, C., Dani, C., Fumagalli, F., Masi, A., Mannaioni, G., 2023. Ethanol-induced AMPA alterations are mediated by mGLU5 receptors through miRNA upregulation in hippocampal slices. Eur. J. Pharmacol. 955. https://doi.org/10.1016/j.ejphar.2023.175878.

Gianoulakis, C., 1990. Rats exposed prenatally to alcohol exhibit impairment in spatial navigation test. Behav. Brain Res. 36, 217–228. https://doi.org/10.1016/0166-4328(90)90060-R.

Godin, E.A., O'Leary-Moore, S.K., Khan, A.A., Parnell, S.E., Ament, J.J., Dehart, D.B., Johnson, B.W., Allan Johnson, G., Styner, M.A., Sulik, K.K., 2010. Magnetic resonance microscopy defines ethanol-induced brain abnormalities in prenatal mice: effects of acute insult on gestational day 7. Alcohol. Clin. Exp. Res. 34, 98–111. https://doi.org/10.1111/j.1530-0277.2009.01071.x.

Gutherz, O.R., Deyssenroth, M., Li, Q., Hao, K., Jacobson, J.L., Chen, J., Jacobson, S.W., Carter, R.C., 2022. Potential roles of imprinted genes in the teratogenic effects of alcohol on the placenta, somatic growth, and the developing brain. Exp. Neurol. 347, 113919. https://doi.org/10.1016/j.expneurol.2021.113919.

Hausser, A., Schlett, K., 2019. Coordination of AMPA receptor trafficking by Rab GTPases. Small GTPases. https://doi.org/10.1080/21541248.2017.1337546.

Hellemans, K.G.C., Sliwowska, J.H., Verma, P., Weinberg, J., 2010. Prenatal alcohol exposure: fetal programming and later life vulnerability to stress, depression and anxiety disorders. Neurosci. Biobehav. Rev. 34, 791–807. https://doi.org/10.1016/J.NEUBIOREV.2009.06.004.

Ilari, A., Curti, L., Petrella, M., Cannella, N., La Rocca, A., Ranieri, G., Gerace, E., Iezzi, D., Silvestri, L., Mannaioni, G., Ciccocioppo, R., Masi, A., 2022. Moderate ethanol drinking is sufficient to alter ventral tegmental area dopamine neurons activity via functional and structural remodeling of GABAergic transmission. Neuropharmacology 203, 108883. https://doi.org/10.1016/j.neuropharm.2021.108883.

Kaminen-Ahola, N., Ahola, A., Flatscher-Bader, T., Wilkins, S.J., Anderson, G.J., Whitelaw, E., Chong, S., 2010a. Postnatal growth restriction and gene expression changes in a mouse model of fetal alcohol syndrome. Birth Def. Res. A. Clin. Mol. Teratol. 88, 818–826. https://doi.org/10.1002/bdra.20729.

Kaminen-Ahola, N., Ahola, A., Maga, M., Mallitt, K.A., Fahey, P., Cox, T.C., Whitelaw, E., Chong, S., 2010b. Maternal ethanol consumption alters the epigenotype and the phenotype of offspring in a mouse model. PLoS Genet. 6, 1000811. https://doi.org/10.1371/journal.pgen.1000811.

Kane, C.J.M., Drew, P.D., 2021. Neuroinflammatory contribution of microglia and astrocytes in fetal alcohol spectrum disorders. J. Neurosci. Res. https://doi.org/10.1002/jnr.24735.

Kietzman, H.W., Everson, J.L., Sulik, K.K., Lipinski, R.J., 2014. The teratogenic effects of prenatal ethanol exposure are exacerbated by sonic hedgehog or Gli2 haploinsufficiency in the mouse. PLoS One 9, 89448. https://doi.org/10.1371/journal.pone.0089448.

Lipinski, R.J., Hammond, P., O'Leary-Moore, S.K., Ament, J.J., Pecevich, S.J., Jiang, Y., Budin, F., Parnell, S.E., Suttie, M., Godin, E.A., Everson, J.L., Dehart, D.B., Oguz, I., Holloway, H.T., Styner, M.A., Johnson, G.A., Sulik, K.K., 2012. Ethanol-induced face-brain dysmorphology patterns are correlative and exposure-stage dependent. PLoS One 7, 43067. https://doi.org/10.1371/journal.pone.0043067.

Lisdahl, K.M., Gilbart, E.R., Wright, N.E., Shollenbarger, S., 2013. Dare to delay? The impacts of adolescent alcohol and marijuana use onset on cognition, brain structure, and function. Front. Psychol. 4. https://doi.org/10.3389/fpsyt.2013.00053.

Louth, E.L., Bignell, W., Taylor, C.L., Bailey, C.D.C., 2016. Developmental ethanol exposure leads to long-term deficits in attention and its underlying prefrontal circuitry. eNeuro 3. https://doi.org/10.1523/ENEURO.0267-16.2016.

Luján, R., Nusser, Z., Roberts, J.D.B., Shigemoto, R., Somogyi, P., 1996. Perisynaptic location of metabotropic glutamate receptors mGluR1 and mGluR5 on dendrites and dendritic spines in the rat hippocampus. Eur. J. Neurosci. 8, 1488–1500. https://doi.org/10.1111/J.1460-9568.1996.TB01611.X.

Matthews, D.B., Simson, P.E., 1998. Prenatal exposure to ethanol disrupts spatial memory: effect of the training-testing delay period. Physiol. Behav. 64, 63–67. https://doi.org/10.1016/S0031-9384(98)00019-5.

Mattson, S.N., Crocker, N., Nguyen, T.T., 2011. Fetal alcohol spectrum disorders: neuropsychological and behavioral features. Neuropsychol. Rev. https://doi.org/10.1007/s11065-011-9167-9.

May, P.A., Keaster, C., Bozeman, R., Goodover, J., Blankenship, J., Kalberg, W.O., Buckley, D., Brooks, M., Hasken, J., Gossage, J.P., Robinson, L.K., Manning, M., Hoyme, H.E., 2015. Prevalence and characteristics of fetal alcohol syndrome and partial fetal alcohol syndrome in a Rocky Mountain Region City. Drug Alcohol Depend. 155, 118–127. https://doi.org/10.1016/j.drugalcdep.2015.08.006.

Mews, P., Egervari, G., Nativio, R., Sidoli, S., Donahue, G., Lombroso, S.I., Alexander, D. C., Riesche, S.L., Heller, E.A., Nestler, E.J., Garcia, B.A., Berger, S.L., 2019. Alcohol metabolism contributes to brain histone acetylation. Nature 574, 717–721. https://doi.org/10.1038/s41586-019-1700-7.

Mira, R.G., Lira, M., Tapia-Rojas, C., Rebolledo, D.L., Quintanilla, R.A., Cerpa, W., 2020. Effect of alcohol on hippocampal-dependent plasticity and behavior: role of glutamatergic synaptic transmission. Front. Behav. Neurosci. https://doi.org/10.3389/fnbeh.2019.00288.

Muggli, E., O'Leary, C., Donath, S., Orsini, F., Forster, D., Anderson, P.J., Lewis, S., Nagle, C., Craig, J.M., Elliott, E., Halliday, J., 2016. Did you ever drink more? A detailed description of pregnant women's drinking patterns. BMC Public Health 16, 1–13. https://doi.org/10.1186/S12889-016-3354-9/FIGURES/1.

Murawski, N.J., Moore, E.M., Thomas, J.D., Riley, E.P., 2015. Advances in diagnosis and treatment of fetal alcohol spectrum disorders: from animal models to human studies. Alcohol Res. Curr. Rev. 37, 97–108.

National Health and Medical Research Council, 2020. Australian Guidelines to Reduce Health Risks from Drinking Alcohol. Australian guidelines to reduce health risks from drinking alcohol, Canberra.

Norman, A.L., Crocker, N., Mattson, S.N., Riley, E.P., 2009. Neuroimaging and fetal alcohol spectrum disorders. Dev. Disabil. Res. Rev. https://doi.org/10.1002/ddrr.72.

O'Leary, C.M., Taylor, C., Zubrick, S.R., Kurinczuk, J.J., Bower, C., 2013. Prenatal alcohol exposure and educational achievement in children aged 8-9 years. Pediatrics 132. https://doi.org/10.1542/peds.2012-3002.

Pappalardo-Carter, D.L., Balaraman, S., Sathyan, P., Carter, E.S., Chen, W.A., Miranda, R. C., 2013. Suppression and epigenetic regulation of MiR-9 contributes to ethanol teratology: Evidence from zebrafish and murine fetal neural stem cell models. Alcohol. Clin. Exp. Res. 37 (10), 1657–1667. https://doi.org/10.1111/acer.12139.

Petrelli, B., Weinberg, J., Hicks, G.G., 2018. Effects of prenatal alcohol exposure (PAE): insights into FASD using mouse models of PAE. Biochem. Cell Biol. https://doi.org/10.1139/bcb-2017-0280.

Popova, S., Lange, S., Probst, C., Gmel, G., Rehm, J., 2017. Estimation of national, regional, and global prevalence of alcohol use during pregnancy and fetal alcohol

syndrome: a systematic review and meta-analysis. Lancet Glob. Health 5, e290–e299. https://doi.org/10.1016/S2214-109X(17)30021-9.
Popova, S., Lange, S., Probst, C., Gmel, G., Rehm, J., 2018. Global prevalence of alcohol use and binge drinking during pregnancy, and fetal alcohol spectrum disorder. Biochem. Cell Biol. https://doi.org/10.1139/bcb-2017-0077.
Popova, S., Charness, M.E., Burd, L., Crawford, A., Hoyme, H.E., Mukherjee, R.A.S., Riley, E.P., Elliott, E.J., 2023. Fetal alcohol spectrum disorders. Nat. Rev. Dis. Prim. 91 (9), 1–21. https://doi.org/10.1038/s41572-023-00420-x.
Provensi, G., Costa, A., Passani, M.B., Blandina, P., 2016. Donepezil, an acetylcholine esterase inhibitor, and ABT-239, a histamine H3 receptor antagonist/inverse agonist, require the integrity of brain histamine system to exert biochemical and procognitive effects in the mouse. Neuropharmacology 109, 139–147. https://doi.org/10.1016/j.neuropharm.2016.06.010.
Puglia, M.P., Valenzuela, C.F., 2009. AMPAR-mediated synaptic transmission in the CA1 hippocampal region of neonatal rats: unexpected resistance to repeated ethanol exposure. Alcohol 43, 619–625. https://doi.org/10.1016/j.alcohol.2009.10.004.
Rani, B., Santangelo, A., Romano, A., Koczwara, J.B., Friuli, M., Provensi, G., Blandina, P., Casarrubea, M., Gaetani, S., Passani, M.B., Costa, A., 2021. Brain histamine and oleoylethanolamide restore behavioral deficits induced by chronic social defeat stress in mice. Neurobiol. Stress 14. https://doi.org/10.1016/j.ynstr.2021.100317.
Ricci, E., Beitawi, S.A., Cipriani, S., Candiani, M., Chiaffarino, F., Viganò, P., Noli, S., Parazzini, F., 2017. Semen quality and alcohol intake: a systematic review and meta-analysis. Reprod. Biomed. Online 34 (1), 38–47. https://doi.org/10.1016/j.rbmo.2016.09.012.
Rubert, G., Miñana, R., Pascual, M., Guerri, C., 2006. Ethanol exposure during embryogenesis decreases the radial glial progenitor pool and affects the generation of neurons and astrocytes. J. Neurosci. Res. 84, 483–496. https://doi.org/10.1002/jnr.20963.
Sanchez, L.M., Goss, J., Wagner, J., Davies, S., Savage, D.D., Hamilton, D.A., Clark, B.J., 2019. Moderate prenatal alcohol exposure impairs performance by adult male rats in an object-place paired-associate task. Behav. Brain Res. 360, 228–234. https://doi.org/10.1016/j.bbr.2018.12.014.
Sathyan, P., Golden, H.B., Miranda, R.C., 2007. Competing interactions between Micro-RNAs determine neural progenitor survival and proliferation after ethanol exposure: evidence from an ex vivo model of the fetal cerebral cortical Neuroepithelium. J. Neurosci. 27 (32), 8546–8557. https://doi.org/10.1523/JNEUROSCI.1269-07.2007.
Shi, S.H., Hayashi, Y., Esteban, J.A., Malinow, R., 2001. Subunit-specific rules governing AMPA receptor trafficking to synapses in hippocampal pyramidal neurons. Cell 105, 331–343. https://doi.org/10.1016/S0092-8674(01)00321-X.
Spadoni, A.D., McGee, C.L., Fryer, S.L., Riley, E.P., 2007. Neuroimaging and fetal alcohol spectrum disorders. Neurosci. Biobehav. Rev. https://doi.org/10.1016/j.neubiorev.2006.09.006.
Stringer, R.L., Laufer, B.I., Kleiber, M.L., Singh, S.M., 2013. Reduced expression ofbrain cannabinoid receptor1(Cnr1) is coupled with an increasedcomplementary micro-RNA (miR-26b) in a mousemodel of fetal alcohol spectrum disorders. Clin. Epigenetics 2013 (5), 14. https://doi.org/10.1186/1868-7083-5-14.
Sulik, K.K., Johnston, M.C., Webb, M.A., 1981. Fetal alcohol syndrome: embryogenesis in a mouse model. Science 214 (80), 936–938. https://doi.org/10.1126/science.6795717.
Takahashi, Y., Yamashita, R., Okano, H., Takashima, K., Ogawa, B., Ojiro, R., Tang, Q., Ozawa, S., Woo, G.H., Yoshida, T., Shibutani, M., 2021. Aberrant neurogenesis and late onset suppression of synaptic plasticity as well as sustained neuroinflammation in the hippocampal dentate gyrus after developmental exposure to ethanol in rats. Toxicology 462. https://doi.org/10.1016/J.TOX.2021.152958.
Tsai, P., Bake, S., Balaraman, S., Rawlings, J., Holgate, R.R., Dubois, D., Miranda, R.C., 2014 Jul 25. 2014. MiR-153 targets the nuclear factor-1 family and protects against teratogenic effects of ethanol exposure in fetal neural stem cells. Biol. Open 3 (8), 741–758. https://doi.org/10.1242/bio.20147765.
Vaglenova, J., Pandiella, N., Wijayawardhane, N., Vaithianathan, T., Birru, S., Breese, C., Suppiramaniam, V., Randal, C., 2008. Aniracetam reversed learning and memory deficits following prenatal ethanol exposure by modulating functions of synaptic AMPA receptors. Neuropsychopharmacology 33, 1071–1083. https://doi.org/10.1038/sj.npp.1301496.
Vermeiren, C., Najimi, M., Vanhoutte, N., Tilleux, S., De Hemptinne, I., Maloteaux, J.M., Hermans, E., 2005. Acute up-regulation of glutamate uptake mediated by mGluR5a in reactive astrocytes. J. Neurochem. 94, 405–416. https://doi.org/10.1111/j.1471-4159.2005.03216.x.
Wang, R., Shen, Y.L., Hausknecht, K.A., Chang, L., Haj-Dahmane, S., Vezina, P., Shen, R. Y., 2019. Prenatal ethanol exposure increases risk of psychostimulant addiction. Behav. Brain Res. https://doi.org/10.1016/j.bbr.2018.07.030.
Wijayawardhane, N., Shonesy, B.C., Vaglenova, J., Vaithianathan, T., Carpenter, M., Breese, C.R., Dityatev, A., Suppiramaniam, V., 2007. Postnatal aniracetam treatment improves prenatal ethanol induced attenuation of AMPA receptor-mediated synaptic transmission. Neurobiol. Dis. 26, 696–706. https://doi.org/10.1016/j.nbd.2007.03.009.
Wijayawardhane, N., Shonesy, B.C., Vaithianathan, T., Pandiella, N., Vaglenova, J., Breese, C.R., Dityatev, A., Suppiramaniam, V., 2008. Ameliorating effects of preadolescent aniracetam treatment on prenatal ethanol-induced impairment in AMPA receptor activity. Neurobiol. Dis. 29, 81–91. https://doi.org/10.1016/J.NBD.2007.08.001.
Wozniak, J.R., Riley, E.P., Charness, M.E., 2019. Clinical presentation, diagnosis, and management of fetal alcohol spectrum disorder. Lancet Neurol. https://doi.org/10.1016/S1474-4422(19)30150-4.
Zerial, M., McBride, H., 2001. Rab proteins as membrane organizers. Nat. Rev. Mol. Cell Biol. https://doi.org/10.1038/35052055.